

1 Article

2 Spatial Gap-Filling of ESA CCI Satellite-Derived Soil 3 Moisture based on Linear Geostatistics

4 Ricardo M. Llamas¹, Mario Guevara¹, Danny Rorabaugh², Michela Taufer² and Rodrigo Vargas^{1*}

5 ¹ University of Delaware, Dept. of Plant and Soil Sciences, Newark, Delaware, USA; rllamas@udel.edu
6 (R.LL.), mguevara@udel.edu (M.G.)

7 ² University of Tennessee, Dept. of Electrical Engineering and Computer Science, Knoxville, Tennessee,
8 USA; dror@utk.edu (D.R.), taufer@utk.edu (M.T.)

9 * Correspondence: rvargas@udel.edu; Tel.: +1-302-831-1386 (R.V.)

10 **Abstract:** Soil moisture plays a key role in the Earth's water and carbon cycles, but acquisition of
11 continuous (i.e., gap-free) soil moisture measurements across large regions is a challenging task due
12 to limitations of currently available point measurements. Satellites offer critical information for soil
13 moisture over large areas on a regular basis (e.g., ESA CCI, NASA SMAP), however, there are
14 regions where satellite-derived soil moisture cannot be estimated because of certain circumstances
15 such as high canopy density, frozen soil, or extreme dry conditions. We compared and tested two
16 approaches--Ordinary Kriging (OK) interpolation and General Linear Models (GLM)--to model soil
17 moisture and fill spatial data gaps from the European Space Agency Climate Change Initiative (ESA
18 CCI) version 3.2 (and compared them with version 4.4) from January 2000 to September 2012, over
19 a region of 465,777 km² across the Midwest of the USA. We tested our proposed methods to fill gaps
20 in the original ESA CCI product, and two data subsets, removing 25% and 50% of the initially
21 available valid pixels. We found a significant correlation coefficient ($r = 0.523$, RMSE = 0.092 m³m⁻³)
22 between the original satellite-derived soil moisture product with ground-truth data from the North
23 American Soil Moisture Database (NASMD). Predicted soil moisture using OK also had significant
24 correlation coefficients with NASMD data, when using 100% ($r = 0.522$, RMSE = 0.092 m³m⁻³), 75%
25 ($r = 0.526$, RMSE = 0.092 m³m⁻³) and 50% ($r = 0.53$, RMSE = 0.092 m³m⁻³) of available valid pixels for
26 each month of the study period. GLM had lower but significant correlation coefficients with
27 NASMD data (average $r = 0.478$, RMSE = 0.092 m³m⁻³) when using the same subsets of available data
28 (i.e., 100%, 75%, 50%). Our results provide support for OK as a technique to gap-fill spatial missing
29 values of satellite-derived soil moisture products across the Midwest of the USA.

30 **Keywords:** Soil Moisture; Remote Sensing; Geostatistics; Gap-Filling; Midwestern USA

31

32 1. Introduction

33 Addressing global environmental challenges requires knowledge and information derived from
34 the most accurate and complete available datasets. Soil moisture has an important role in the water
35 and energy cycles, and is regarded as one of the essential terrestrial climate variables [1] due to its
36 influence in soil and atmosphere feedbacks. Furthermore, soil moisture is a critical input variable for
37 applications such as climate modeling [2–4], agricultural planning [5,6], and carbon budget analyses
38 [7,8]. Because of the importance of soil moisture, there are many in situ monitoring networks,
39 organized at the global [9], regional [10,11], or national-scale [12–15]. Despite these national to global
40 efforts, there is still a challenge to represent spatially explicit soil moisture information across large
41 regions related to spatial limitations of point measurements.

42 Soil moisture can be estimated using remote sensors (e.g., spaceborne radiometers and radar
43 sensors) to provide coarse-scale estimates on a regular basis [9,16]. Examples of remote sensing soil
44 moisture monitoring systems include NASA's Soil Moisture Active Passive (SMAP) [16], ESA's Soil
45 Moisture and Ocean Salinity (SMOS) [17] and the European Space Agency Climate Change Initiative
46 (ESA CCI) [11,18] that deliver publicly available data for a wide range of applications. Despite

47 advances in remote sensing technology, there are still large areas where soil moisture information is
48 not regularly acquired, yielding information gaps in time and space across the world. Missing
49 information arises from certain circumstances such as high canopy density, snow and ice cover,
50 extremely dry surface conditions or frozen soil [11]. These factors hinder radiometers or radar sensors
51 in measuring the dielectric constant in the top layer of soil in order to estimate water content [19].

52 Consequently, there is a need to develop gap-filling strategies to provide spatially complete
53 satellite-derived soil moisture data across the world. In the most recent version of the ESA CCI
54 product (version 4.4), active and passive sensors are combined by means of a weighted mean, being
55 proportional to the signal-to-noise ratio (SNR) [20]. These ratios are estimated using Triple
56 Collocation Analysis, which is a method that estimates random error variances of three collocated
57 datasets of soil moisture estimates [21]. In areas, where no triple collocation analysis estimates are
58 available, soil moisture values are estimated using a polynomial regression between the signal-to-
59 noise ratios [20]. Other statistical methods (e.g., discrete cosine transformations and singular
60 spectrum analysis) have been applied to fill spatial gaps for satellite-derived geophysical datasets, as
61 well as soil moisture from field measurements [22,23]. These approaches are focused either on the
62 statistical distribution of the data, or in three-dimension information, which includes both space and
63 time. We postulate that alternative gap-filling methods could take advantage on the information
64 contained in the spatial distribution of soil moisture or its relationship with key geophysical
65 variables, such as temperature and precipitation which have been identified in other studies [3,9,24].

66 In this research, we propose to test the performance of two methods to gap-fill satellite-derived
67 soil moisture in ESA CCI product version 3.2, in which no further gap-filling techniques have been
68 applied. Although version 4.4 includes a gap-filling strategy (as described above), this version still
69 contains gaps across many regions of the world. Our approaches aim to offer alternative strategies to
70 offer spatially complete soil moisture estimates, other than the methods applied in ESA CCI product
71 version 4.4 [21].

72 We tested two approaches. The first one is based on Ordinary Kriging (OK) spatial interpolation
73 [25–27] to take advantage of the spatial autocorrelation of satellite-derived soil moisture on gridded
74 surfaces. The second one is based on the application of General Linear Models (GLM) to explore the
75 relationship between soil moisture (response variable) with precipitation and minimum air
76 temperature (explanatory variables). We tested these two methods because OK has the advantage of
77 requiring solely spatial soil moisture data, and GLM has the advantage of benefiting from the
78 incorporation of geophysical covariates.

79 We focused our study over a region in the Midwestern United States (with abundant satellite-
80 data estimates and in situ measurements) between 2000 and 2012. We evaluated the outcome of our
81 gap-filling approaches with ground-truth information using *in situ* measurements from the North
82 American Soil Moisture Database (NASMD) [15]. Although we present monthly results for both OK
83 and GLM, overall correlation coefficient with field data for the period of this study shows that OK
84 performed better than GLM, using as reference the correlation coefficient (e.g. Pearson) between
85 original satellite estimates and ground-truth data from NASMD. In addition to other techniques
86 aimed to gap-filling in satellite-derived geophysical datasets [22,23], our results highlight the
87 potential of spatial interpolation to offer spatially complete soil moisture information. Furthermore,
88 methods based on the spatial distribution of soil moisture, such as OK, might compensate for the lack
89 of geophysical covariates information such as precipitation and air temperature in different regions
90 across the world.

91 Section 2 provides a description of the region of interest as well as the parameters to select our
92 time frame. Data acquisition, preprocessing, selection of the geophysical covariates, application of
93 proposed gap-filling approaches and validation strategy are also described in Section 2. Section 3
94 describes the performance of both OK and GLM techniques, as well as the results of cross-validation
95 for both models. Validation using reference correlation between original satellite data and ground-
96 truth soil moisture information is also described in Section 3 and compared with models outputs.
97 Section 3 finally shows the capability of our methods to reproduce the spatial soil moisture patterns
98 shown by the original ESA CCI product. Section 4 proceeds with the discussion of our findings and

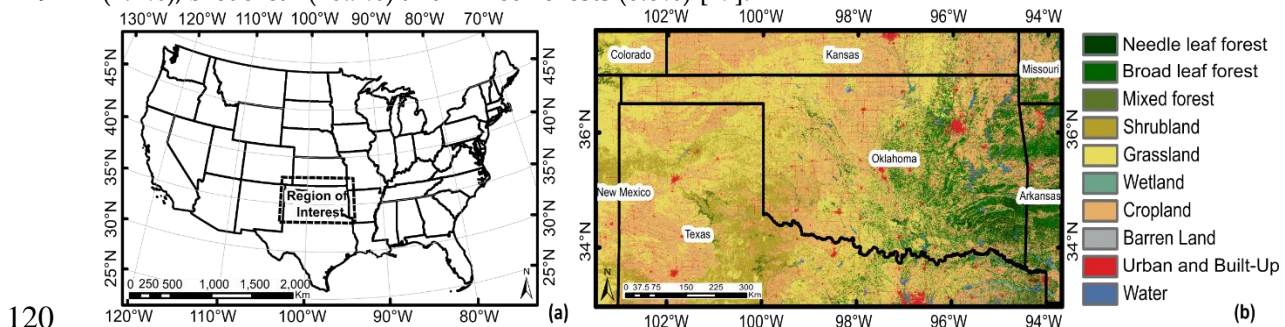
99 their implications in providing spatially complete soil moisture information derived from ESA CCI
 100 satellite estimates, version 3.2. Section 5 summarizes important remarks of our work and its
 101 implications in providing soil moisture information for specific applications.

102 2. Materials and Methods

103 2.1. Region of Interest

104 The selected region of interest was an area of 465,777 km² (Figure 1a) centered in the state of
 105 Oklahoma (180,986 km²) and covering some areas of surrounding states within Midwestern USA:
 106 Texas (159,489 km²), Colorado (11,210 km²), Kansas (61,343 km²), Missouri (10,844 km²), New Mexico
 107 (18,550 km²) and Arkansas (23,356 km²). The region of interest shows a variety of environmental
 108 conditions, both natural and human-driven, that allowed us to test the spatial performance of our
 109 gap-filling frameworks. This diversity mitigates bias due to specific environmental conditions (e.g.,
 110 homogenous land cover, uniform topographic features), which are not the attention of this present
 111 study. The region of interest for this study was selected in response to the availability of ground-truth
 112 data in that area, mainly over Oklahoma, where MESONET provides a robust set of historical soil
 113 moisture records [28]. Additionally, soil moisture data availability in northern Texas and the
 114 remaining areas in the region of interest are consistently represented by the NASMD. We highlight
 115 that the NASMD integrates data from several monitoring networks including MESONET [15].

116 The region of interest (Figure 1a) includes a wide variety of land cover types (Figure 1b)
 117 dominated by grassland (35.5%), cropland (31.9%) and shrubland (11.0%) in the central and western
 118 areas. Whereas forested areas are mostly located in the eastern portion, distributed across needleleaf
 119 (2.2%), broadleaf (10.9%) and mixed forests (0.6%) [29].



120
 121 **Figure 1.** (a) Region of interest in the Midwestern USA, where soil moisture gap-filling methods were
 122 performed; (b) Land cover types over the region of interest (30 m), level 1 NALCMS classification
 123 [29].

124 2.2. Data

125 2.2.1. Satellite-Derived Soil Moisture

126 For this study, we used the ESA CCI soil moisture product version 3.2 (Table 1) that has gathered
 127 historical records from active and passive remote sensors [11,18]. This product provides soil moisture
 128 estimates at 0.25 degrees of spatial resolution on a daily basis, from November 1978 to December
 129 2016. Passive sensors were used to generate this product up to 1991, and the combination of both
 130 active and passive sensors was incorporated since then [11]. The ESA CCI product was developed in
 131 collaboration with Vienna University of Technology (TU Wien) and focuses on the use of data derived
 132 from C-band scatterometers. Such as European Remote Sensing Satellites (ERS-1/2) and METOP, as
 133 well as the use of data from multi-frequency radiometers such as Scanning Multichannel Microwave
 134 Radiometer (SMMR), Special Sensor Microwave Imager (SSM/I), Microwave Imager (TMI),
 135 Advanced Microwave Scanning Radiometer (AMSR-E) and Windsat [3]. These sensors are
 136 characterized for the suitability for soil moisture retrieval [3].

137 ESA CCI soil moisture product version 3.2 has not been subject to any further gap-filling
 138 technique (as compared to version 4.4), and represents a suitable product for testing the proposed

139 satellite-derived soil moisture gap-filling approaches in this work. Although version 4.4. does mask
 140 areas of dense vegetation using Vegetation Optical Depth Layers, as well as flag measurements taken
 141 under frozen conditions [21], the product still shows a large number of gaps in our region of interest.
 142 Additional analyses of our approaches applied to ESA CCI soil moisture version 4.4 are described in
 143 supplementary material (S1).

144

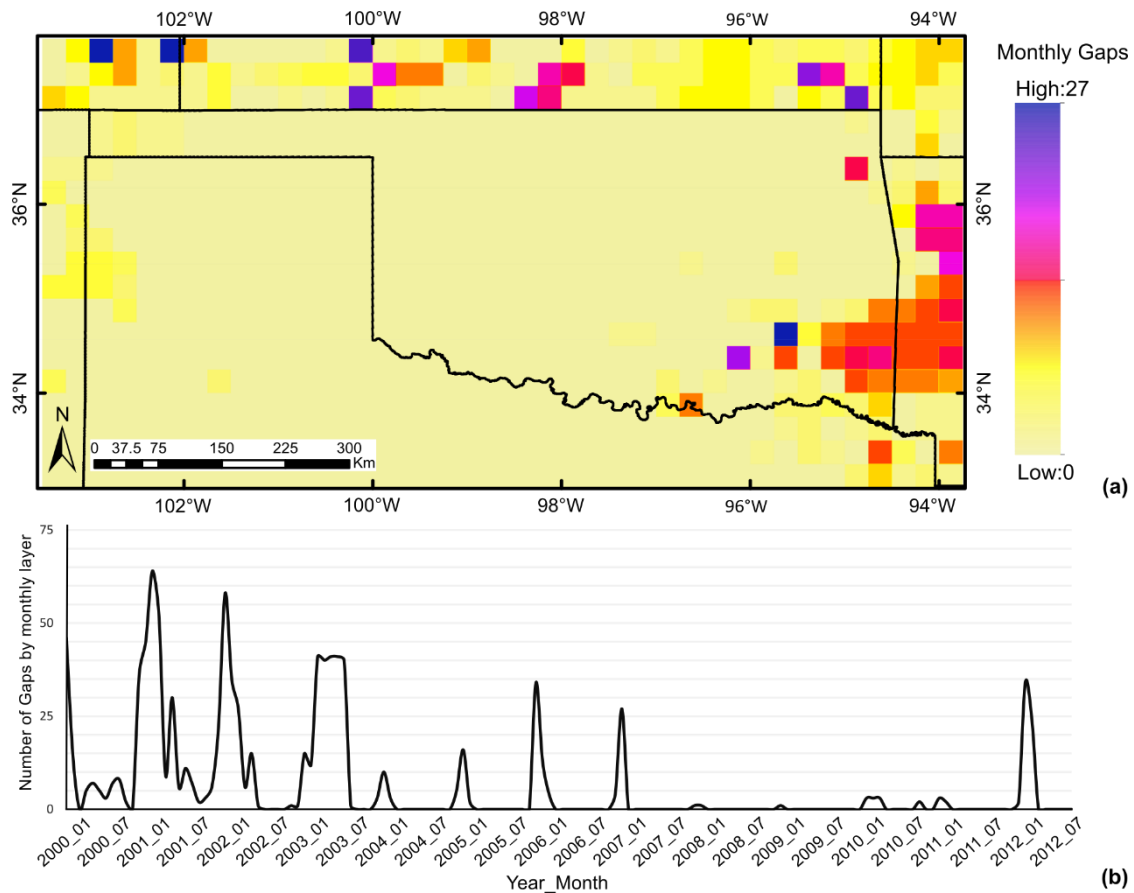
Table 1. Main characteristics of ESA CCI soil moisture version 3.2 [18].

Title ESA CCI Soil Moisture Version 3.2	
Release date	February 2017
Available products	Active
	Passive
	Combined
Scatterometer sensors used	ERS- 1/2 AMI WS
	ERS-2 AMI WS
	MetOp-A + B ASCAT
	SMMR
	SSM/I
Radiometer sensors used	TMI
	Windsat
	AMSR-E
	AMSR2
Available time span	SMOS
	November 1978 - December 2015 (Active and Passive products)
	August 1991 - December 2015 (Active product)

145

146 Daily soil moisture global records from the ESA CCI product were acquired and then cropped to
 147 the region of interest. Daily estimates were merged into monthly soil moisture spatial layers using mean
 148 and median values, this way; we tackled the lack of daily coverage in areas out of the satellites swath.
 149 Monthly mean values initially reduced the number of gaps in daily products but still provided
 150 reliable information to identify spatial patterns and trends in our study period. These values then
 151 were used to explore their relationship with different geophysical covariates (supplementary material
 152 S2). Monthly values can describe soil moisture variability over a few weeks due to soil moisture
 153 memory effects, as water content derived from sudden excessive rains or lack of water onset, can
 154 generate wetness or dryness conditions that might last for a couple of weeks [2].

155 An important step in preparing the soil moisture data for analysis is identifying the most relevant
 156 summary statistics, such as mean or median. The median value is more useful when data is
 157 concentrated on a brief period of the month (because of long data gaps) with an uneven distribution of
 158 data [30]. However, mean monthly soil moisture values showed higher correlation with the tested set
 159 of geophysical covariates (supplementary material S2). For our study period (January 2000 to
 160 September 2012), Figure 2 shows the frequency of spatial and temporal monthly soil moisture data gaps,
 161 where no mean values were calculated due to lack of valid pixels. A pixel is considered valid when soil
 162 moisture estimates are available from the ESA CCI product over the region of interest.



163

164

165 **Figure 2. (a)** Number of gaps in monthly soil moisture estimates over the region of interest, derived

166 from ESA CCI product (version 3.2), January 2000 – September 2012; **(b)** Distribution of gaps along

167 the study period in monthly steps, each number represents the quantity of pixels without data, out of

167 741 pixels in the region of interest.

168 2.2.2. Soil Moisture Covariates

169 For the ESA CCI gap-filling approach using GLM, we explored the relationships between soil
 170 moisture and some geophysical variables. Ancillary monthly layers were generated for precipitation,
 171 atmospheric temperature, as well as static values of soil texture and topographic wetness index
 172 (TWI). These selected variables are known to work as drivers for water input in soil [2,3].

173 Meteorological data was acquired at 1-km spatial resolution monthly layers produced by the
 174 Daily Surface Weather and Climatological Summaries (DAYMET) [31]. Total monthly precipitation,
 175 as well as monthly averages of minimum and maximum air temperature raster layers from January
 176 2000 to September 2012 were cropped to the region of interest, projected to the WGS84 Lat-Long
 177 coordinate system and resampled to 0.25 degrees by means of nearest neighbor method (ngb) [32].

178 Soil texture was obtained from the US soil survey geographic database [33] and we classified all
 179 classes into four general categories based on the texture triangle from US Department of Agriculture
 180 (USDA) [34]: coarse, medium, medium fine, and fine. Soil texture then was resampled to 0.25 degrees
 181 resolution using ngb [32]. We calculated TWI using SAGA GIS [35] with a digital elevation model at
 182 250 meters resolution [25], then resampling the output to 0.25 degrees using ngb [32]. Detailed
 183 information on the definition of geophysical variables for this work and their further processing are
 184 given in the supplementary material (supplementary material S2).

185 2.2.3. Validation Data

186 In order to establish a reference value that describes the spatial distribution pattern of soil
 187 moisture over our region of interest, we acquired records from the North American Soil Moisture
 188 Database (NASMD). NASMD provides the densest possible soil moisture network that integrates

189 field measurements across North America [15]. By 2015, the NASMD had integrated 33 observation
190 networks and two short-term soil moisture campaigns, providing ground-truth data for over 1,800
191 observation sites in the USA, Canada and Mexico [15]. Some of the densest regional networks
192 integrated by NASMD offer soil moisture data in our region of interest (e.g., MESONET), and records
193 at 5-cm depth, where the soil layer closely interacts with the atmosphere and it is sensed by satellites
194 [36]. We extracted all information available from the NASMD over our region of interest that
195 comprised records at 5-cm depth, from January 2000 to September 2012. Finally, we transformed this
196 data to georeferenced point layers to be integrated in our ground-truth validation approach.

197 2.3. Gap-filling Methods

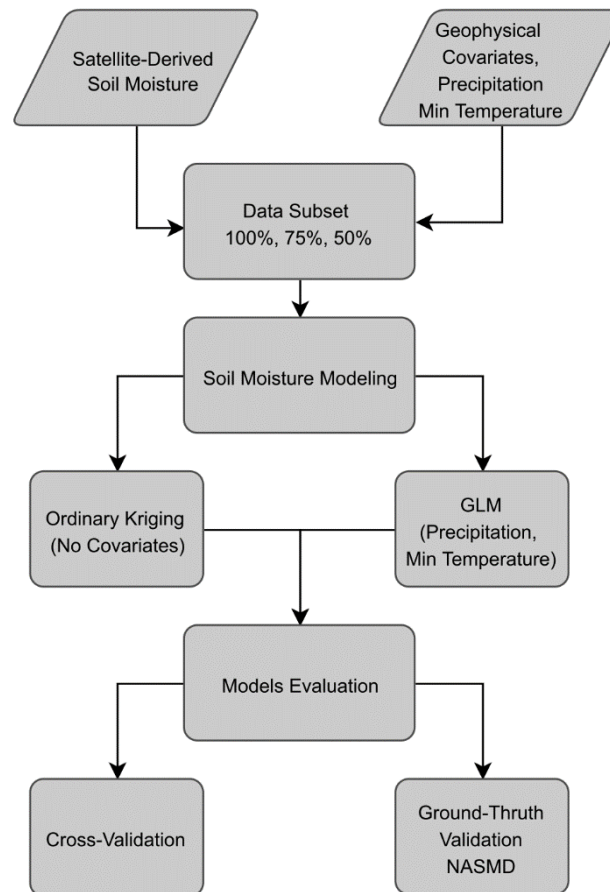
198 Our first gap-filling approach was based on OK interpolation. This technique lead to high
199 uncertainty over areas with very large spatial gaps because it relies on the spatial autocorrelation of
200 available data. Consequently, we also tested a second approach based on GLM to test the relationship
201 between soil moisture and geophysical covariates.

202 OK interpolation strategy depends solely on separation distance between sampled locations and
203 not on an absolute position [27]. This offers a feasible strategy to fill spatial gaps in areas where no
204 other information is available to be included in similar interpolation methods such as CoKriging or
205 Regression Kriging. This is the most popular among all Kriging methods, as it works in almost any
206 situation and its assumptions are easily filled [27].

207 General Linear Models (GLM) on the other hand, represent multivariate regression models [37].
208 In this approach, we assume linear relationships between the dependent variable (soil moisture) and
209 the predefined predictors (precipitation, minimum air temperature) before considering relationships
210 that are more complex. These relationships have been also explored in previous studies, integrating
211 predictors such as vegetation indices, precipitation and temperature [38,39].

212 Soil moisture spatial-gaps in the region of interest are not always sufficient to test interpolation
213 methods, as in some months there are no gaps over the region of interest. Thus, we decided to randomly
214 remove valid data from each soil moisture monthly layer as well as their correspondent locations on
215 the geophysical covariates layers. Then both OK and GLM were performed on 100%, 75% and 50% of
216 available valid pixels in each month, similar to gap-filling analyses in previous studies [22].

217 The overall process for soil moisture prediction (Figure 3), derived from the proposed modeling
218 techniques, was evaluated using cross-validation and ground-truth data from the NASMD available
219 from January 2000 to September 2012. An extensive description of workflow as well as a sample
220 process for one month are provided in supplementary material (S3).
221



222

223

224

225

Figure 3. Workflow for soil moisture modeling and the gap-filling over the region of interest, regarding 100%, 75% and 50% of available valid pixels in each monthly layer. Cross-validation as well as ground-truth validation is also described.

226

2.3.1. Ordinary Kriging

227

228

229

230

231

232

233

OK was performed using the AutoMap package developed for R statistical platform [40]. By

234

235

236

237

238

239

240

241

242

243

means of the autofit-variogram tool, the best-fitted variogram model was automatically selected to generate independent predictions over each month. Five different variogram models (i.e., Spherical, Exponential, Gaussian, Matern and Stein's parameterization) were evaluated and the one with the smallest residual sum of the squares was selected [40]. The prediction of values at unsampled locations is the linear combination of N variables, as expressed in Equation 1,

$$Z(u) = \sum_{i=1}^N \lambda_i Z(u_i) \quad (1)$$

where λ_i represents the original weighted values. Weights are calculated as function of distance between sampled and unsampled locations to be predicted. The weights sum must be equal to 1, thus estimations fulfill unbiasedness requirement [41],

After OK spatial interpolation, predicted values as well as their standard errors were obtained for each month, derived in three different cases from 100%, 75% and 50% of available valid pixels. We applied 10-fold cross-validation [40] to OK outputs, for the above mentioned percentages of valid pixels using autoKrigcv [40]. Finally, we assessed the spatial dependence found in each monthly layer using the nugget-sill ratio. Ratios of at most 0.25 represented strong spatial dependence, between 0.25 and 0.75 moderate spatial dependence, and at least 0.75 weak spatial dependence, as previously reported [42].

244

2.3.2. General Linear Models

245

246

247

For GLM, we first tested the overall correlation between soil moisture (monthly mean and median values) and each one of the geophysical covariates (monthly precipitation, monthly maximum and minimum air temperature, soil texture and TWI). Secondly, we extracted a time series

248 for each valid pixel along the 153 monthly soil moisture layers, and tested the pixel-individual
249 correlation with each one of the covariates. Finally, we calculated the correlation coefficients of all
250 valid pixels available for each monthly layer with the corresponding temporal layer for each one of
251 the covariates. Based on these analyses we established that the spatial values of mean monthly
252 precipitation and minimum air temperature were the variables with the highest absolute correlation
253 coefficient with mean monthly soil moisture (supplementary material S2). These geophysical
254 covariates were used to predict soil moisture based on GLM, as shown in Equation 2,

$$255 Y_i = \beta_0 + \beta_1 X_{i1} + \beta_2 X_{i2} + \varepsilon_i \quad (2)$$

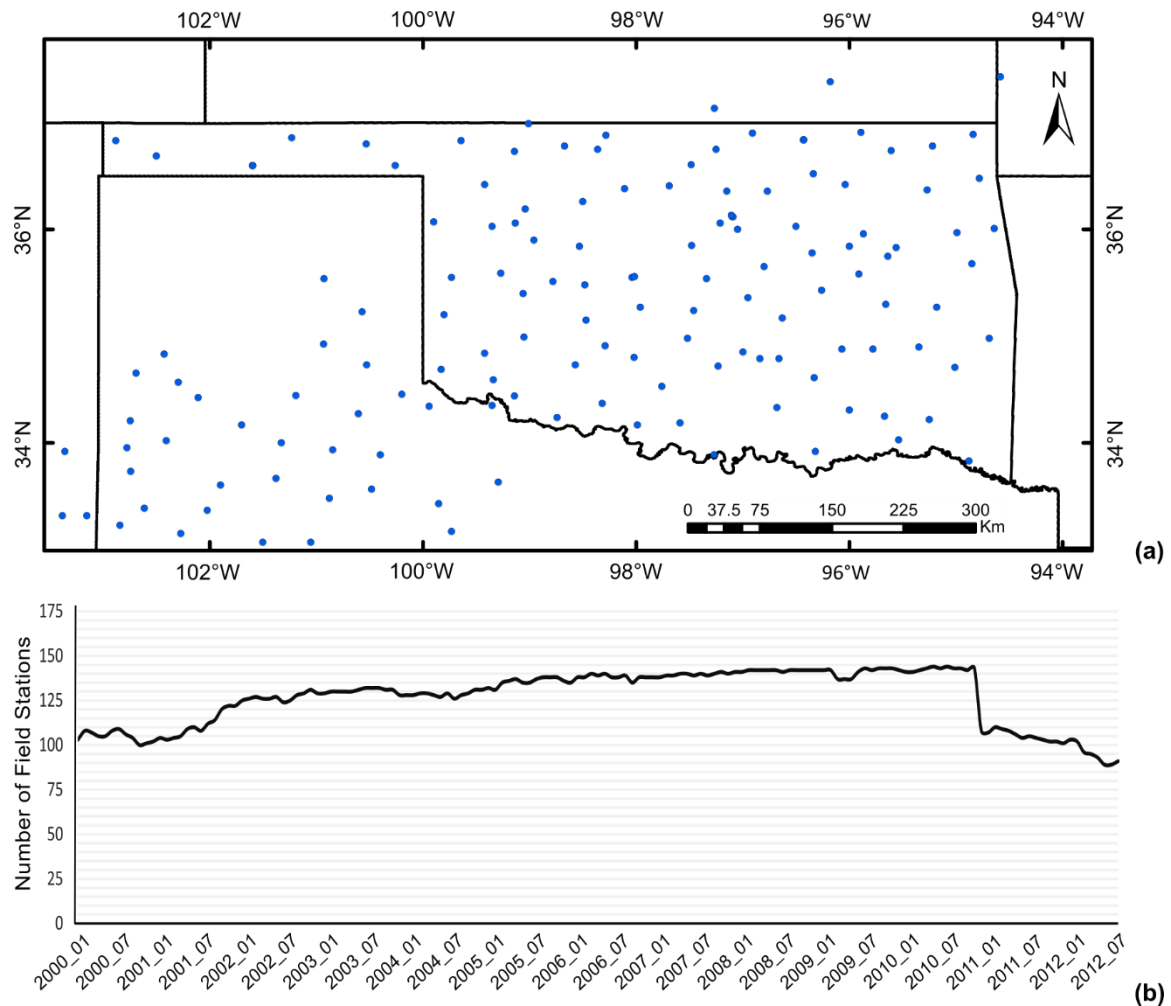
256 where Y_i represents the response variable, X_{i1} and X_{i2} represent the predictor variables, β_0 , β_1
257 and β_2 are the parameters of the model, and ε_i is the error term [37].

258 Predictions were also performed for the three predefined subsets (100%, 75% and 50%) of
259 available valid data over the region of interest in each month of the study period. We used the GLM
260 tool from caret statistical package in R [43] to generate independent models for each month, as well
261 as a 10-fold cross-validation process. For this purpose, we used 75% of the data in each independent
262 monthly dataset as training data and 25% as test data.

263 2.4. Ground-Truth Validation

264 2.4.1. Reference correlation between NASMD and satellite-derived soil moisture

265 First, we established a reference correlation value between original satellite-derived soil
266 moisture and data from the NASMD. We extracted all available data from NASMD over the region
267 of interest for each month during the study period and calculated the mean monthly value of soil
268 moisture at 5-cm depth, for each field station. Thus, capturing as much variation as possible from the
269 upper soil layers sensed by the satellites. We tested the correlation between satellite-derived values
270 over each spatially correspondent pixel with soil moisture information derived from the NASMD.
271 This process was performed over the layers using 100%, 75% and 50% of available valid pixels. When
272 there was more than one NASMD station within one corresponding pixel of satellite-derived soil
273 moisture, every station value from within the pixel area was accounted for the correlation analysis
274 with the satellite data. Overall, we used data from 144 stations in the months with the highest
275 availability of field soil moisture records. The use of all NASMD available stations allowed us to
276 retain the overall observation-estimation pairs. Figure 4 shows the number of available NASMD
277 stations available over the region of interest in each month. Across the entire study period, all
278 available stations provided 19,336 points to compare satellite-derived soil moisture estimates and
279 ground-truth data.



280

281

282

283

Figure 4. All NASMD stations available for the study period (144); (a) Stations are broadly distributed over Oklahoma and northern Texas, however, ground-truth data is scarce over the surrounding states within the region of interest; (b) Number of ground-truth stations available per month for validation.

284

2.4.2. Correlation between predicted soil moisture and NASMD

285

286

287

288

289

290

291

292

In order to validate our soil moisture predicted values, we looked for the closest similar correlation coefficient from our outputs and the NASMD, to the correlation coefficient between the original ESA CCI estimates with NASMD. Thus, repeating the same value of a satellite estimate or predicted value for each field station that is located within the same cell. This way we take advantage of as much validation information as possible over our region of interest. We followed the same approach as in section 2.4.1 to evaluate the soil moisture values derived from the modeling approaches with the NASMD. This allowed us to evaluate 19,411 pixels where we calculated the overall correlation coefficient (all months), and monthly correlation coefficients.

293

3. Results

294

3.1. OK models selected for soil moisture predictions

295

296

297

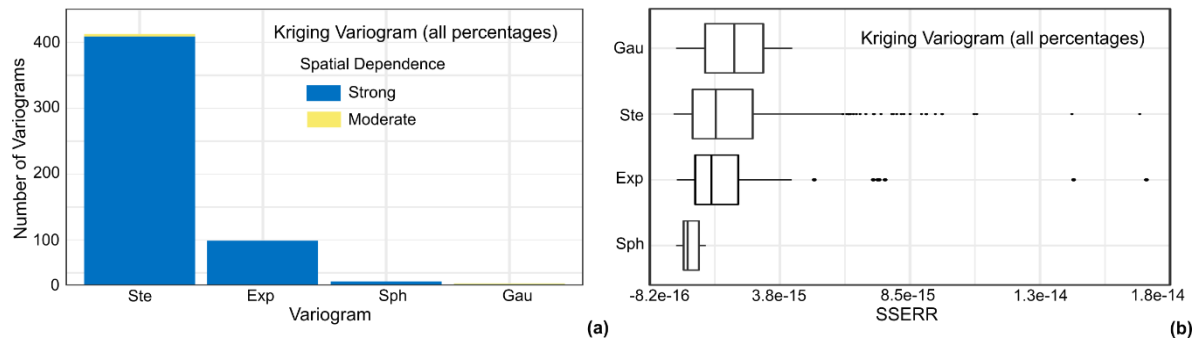
298

299

300

301

Variograms using Stein's parameterization [44] were the most common across the 459 monthly layers (n=382). Exponential (n=69), Spherical (n=6), and Gaussian (n=2) were used in a substantially lower number of predicted soil moisture layers. We found strong spatial dependence in 454 of the monthly layers (nugget-sill < 0.25) and moderate spatial dependence in the remaining 5 layers (0.25 < nugget-sill < 0.75) (Figure 5a). Stein's parameterization [44] had an overall relatively small sum of squared errors when compared to most variogram models and when considered the large sample size (Figure 5b).



302

303

304

305

Figure 5. (a) Most fitted variogram models used to predict soil moisture, 459 models generated for 153 monthly layers derived from all percentages (100%, 75% and 50%) of valid pixels; (b) Boxplots of the sum of squared error (SSERR) for each set of variogram model.

306

3.2. Cross-Validation of predicted values

307

308

309

Overall, both models had good cross-validation results, but OK had consistently higher correlation coefficients and lower RMSE (Table 2). These results were consistent as different percentage of available data was used.

310

311

Table 2. Cross-validation outputs for OK and GLM, all predicted and observed values along the 153 monthly layers.

Method	Percentage of data	Correlation	RMSE
OK	100%	0.968	0.012 m ³ m ⁻³
	75%	0.967	0.012 m ³ m ⁻³
	50%	0.963	0.013 m ³ m ⁻³
GLM	100%	0.813	0.028 m ³ m ⁻³
	75%	0.813	0.028 m ³ m ⁻³
	50%	0.814	0.028 m ³ m ⁻³

312

313

314

315

316

317

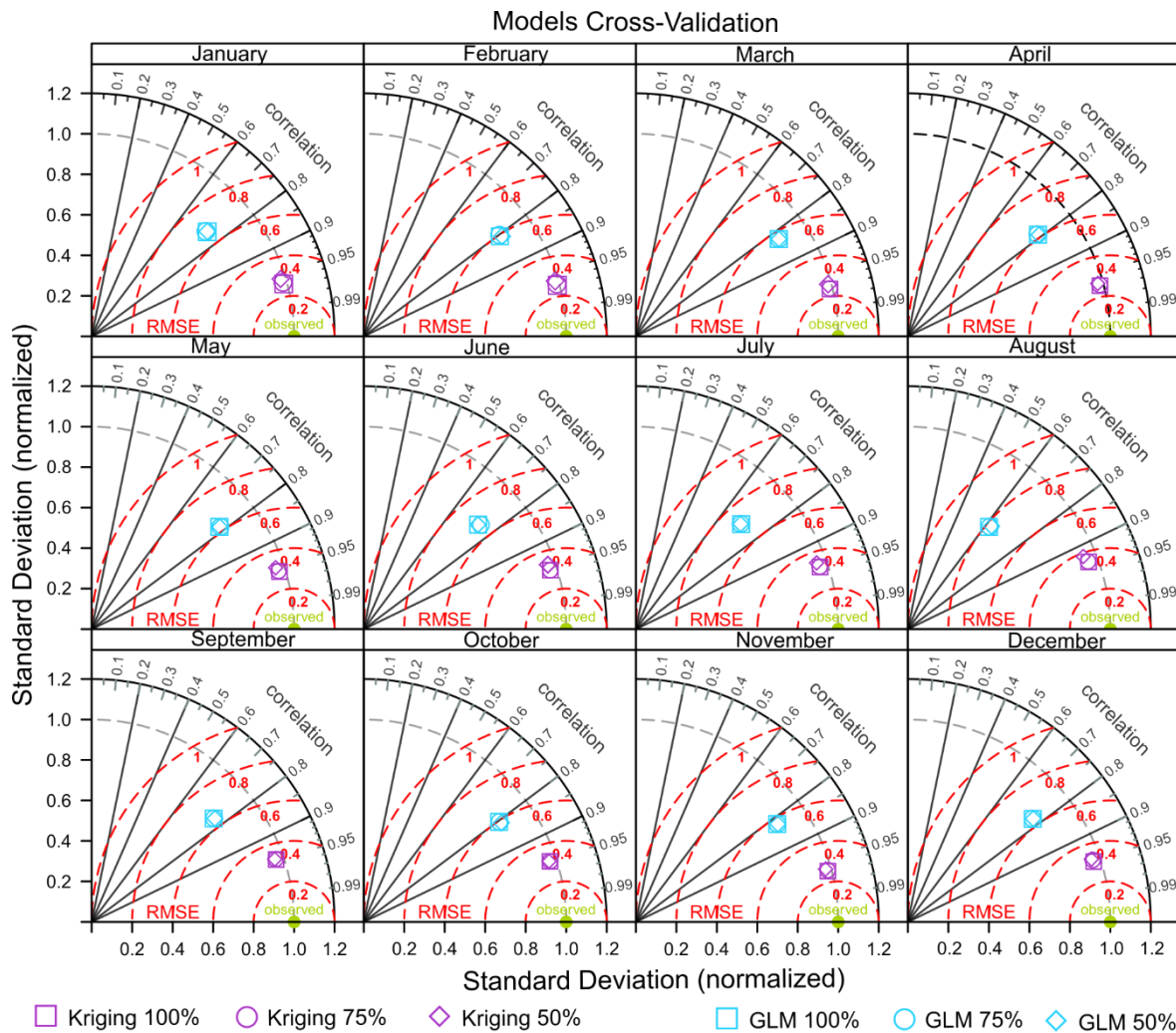
318

319

320

321

Additional cross-validation between predicted and observed values by month (January-December) is reported using Taylor diagrams (Figure 6), which simultaneously report correlation coefficient, normalized standard deviation and centered root mean squared error [45]. The Taylor diagrams [46] consistently show that OK had higher correlation coefficient and lower centered RMSE and standard deviations, and consequently were closer to the observations. These results were consistent regardless the percentage of available data used. Overall, OK had correlation coefficients ranging from 0.924 to 0.971, whereas GLM values ranged between 0.618 and 0.83. Centered RMSE values between observed and predicted values with OK ranged between 0.227 and 0.377, whereas GLM ranged between 0.558 and 0.786.



322 □ Kriging 100% ○ Kriging 75% ◇ Kriging 50% □ GLM 100% ○ GLM 75% ◇ GLM 50%

323 **Figure 6.** Taylor diagrams based on Cross-validation by month across years, OK and GLM using
324 100%, 75% and 50% of available valid data. Standard deviation and RMSE values for each output have
325 been normalized using the standard deviation of the observed values.

326 3.3. Ground-Truth Validation with NASMD

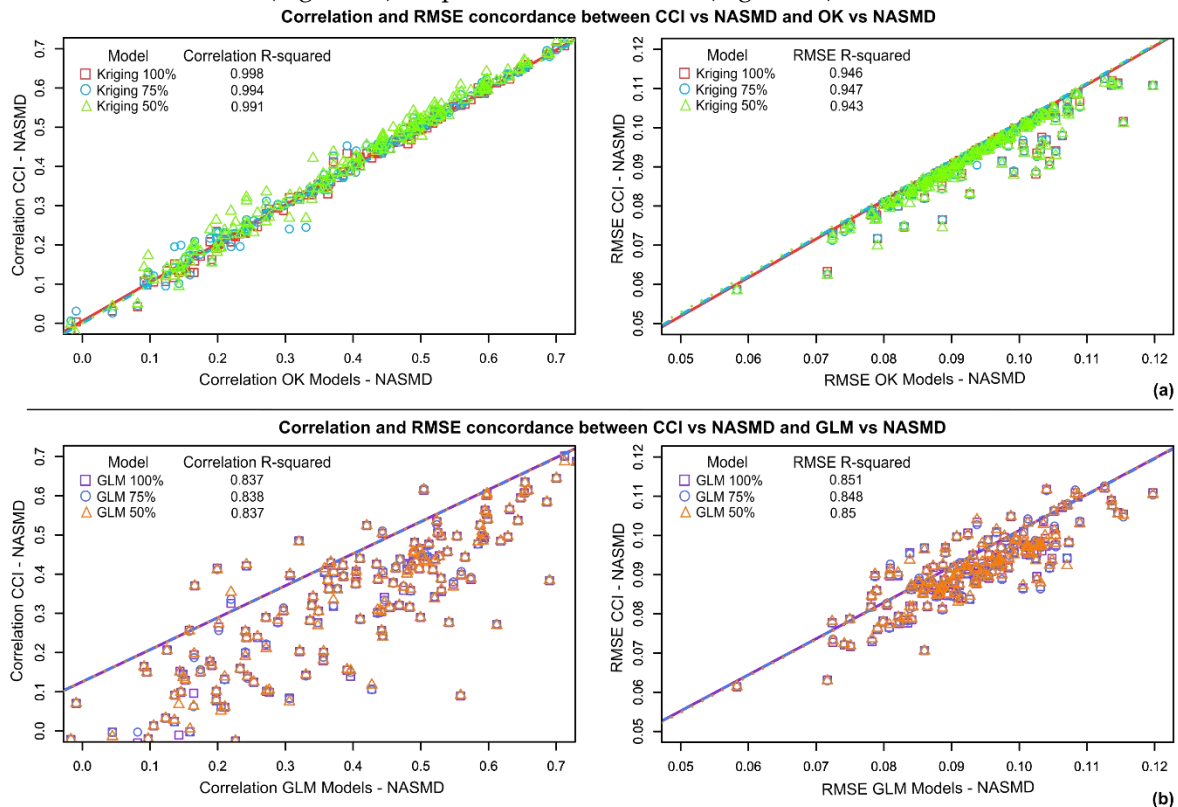
327 We found an overall correlation coefficient of $r = 0.523$ and a RMSE of $0.093 \text{ cm}^3 \text{ cm}^{-3}$ between
328 the original ESA CCI data and the available NASMD stations across the study period (153 months).
329 These values served as baseline and showed that values generated using OK were closer to the
330 reference than those using GLM (Table 3).

331 **Table 3.** Overall correlation coefficients between all ground-truth validation points and CCI soil
332 moisture product, as well as gap-filled outputs. Percentages show the data subset used to predict
333 soil moisture values over the region of interest.

Method	Percentage of data	Correlation	RMSE
CCI	100%	0.523	0.092 m^3m^{-3}
	100%	0.522	0.092 m^3m^{-3}
	OK	75%	0.526
OK	50%	0.530	0.092 m^3m^{-3}
	100%	0.478	0.092 m^3m^{-3}
	GLM	75%	0.478
50%		0.478	0.092 m^3m^{-3}

334

335 We explored the temporal dynamics of the correlation coefficients and RMSEs by month
 336 throughout the study period. Figure 7 shows the R-squared values between the monthly correlation
 337 coefficients from ground-truth data and CCI products, and coefficients from ground-truth data and
 338 predicted values by both OK and GLM. RMSE is reported in the same manner (Figure 7).
 339 Consistently, OK correlation coefficients with ground-truth data, are closer to correlation coefficients
 340 used as reference between validation data and CCI product (Figure 7a). On the other hand, GLM
 341 outputs show lower general R-squared values between the outputs and the reference, and are hardly
 342 fitted to the regression line (Figure 7b). In a similar way, R-squared between RMSE values from CCI
 343 product and ground-truth data, as well RMSE from model outputs and ground-truth data, show
 344 closer relation for OK (Figure 7a) outputs rather than GLM (Figure 7b).

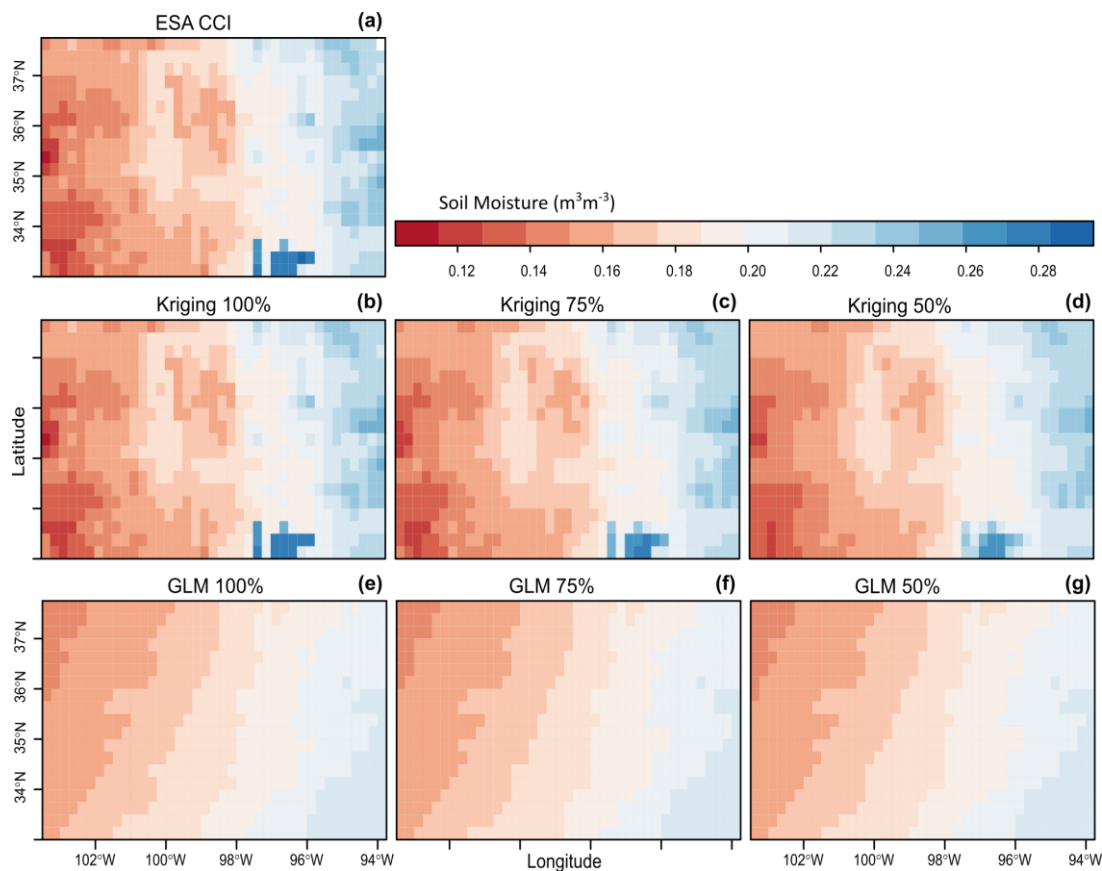


345
 346 **Figure 7.** R-squared values showing the concordance between the reference validation (CCI-NASMD)
 347 and the validation of proposed gap-filling methods with NASMD. Each point represents one month,
 348 using 100%, 70%, or 50% of the available data, with the percentage indicated by the shape used. (a)
 349 Validation of Kriging with NASMD, with correlation on the left and RMSE on the right; (b) Validation
 350 of GLM with NASMD, with correlation on the left and RMSE on the right. Regression lines between
 351 correlated datasets are shown in each plot.

352 3.4. Spatial Gap-Filling performance of modeling methods

353 The comparison between the outputs of our modeling methods in contrast with the original ESA
 354 CCI soil moisture product shows that OK approach better reproduces the spatial pattern captured by
 355 satellite estimates. Figure 8a shows the mean soil moisture estimates from ESA CCI product derived
 356 from 153 monthly layers in our region of interest, without any gap-filling technique. In comparison
 357 to the original spatial distribution of soil moisture, OK visually shows a more similar patterns,
 358 independently of the percentage of valid pixels used for modeling (Figure 8b,c,d). On the other hand,
 359 GLM clearly shows a less effective performance in reproducing soil moisture spatial patterns,
 360 regardless the percentage of valid pixels included in the modeling process (Figure 8e,f,g). We also
 361 found that density distribution that depicts the mean soil moisture values along the study period in
 362 the original ESA CCI is better reproduced by our OK approach. The performance of OK is similar,
 363 either using 100% 75% or 50% of available valid data (Figure 9a). Meanwhile, GLM density

364 distribution falls apart from the values showed in the original ESA CCI product (Figure 9b). By means
 365 of this analysis we confirm the better performance of OK, not only in a direct modeling approach
 366 (Figure 6) and its better relationship with validation data (Figure 7), but also its higher capacity in
 367 reproducing original ESA CCI spatial soil moisture patterns.



368

369

370

371

372

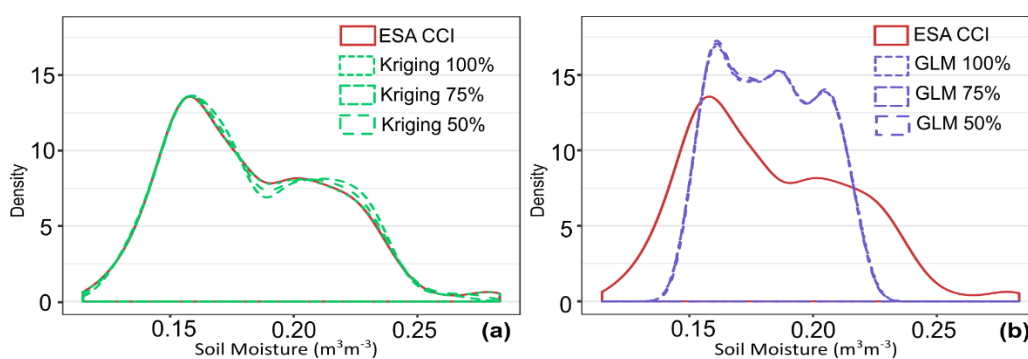
373

374

375

376

Figure 8. Mean soil moisture values along the study period (January 2000 – September 2012) over the region of interest. (a) Mean values of original ESA CCI soil moisture estimates, no gap-filling methods applied; (b) Soil moisture mean values modeled using OK and 100% of available valid data; (c) Soil moisture mean values modeled using OK and 75% of available valid data; (d) Soil moisture mean values modeled using OK and 50% of available valid data; (e) Soil moisture mean values modeled using GLM and 100% of available valid data; (f) Soil moisture mean values modeled using GLM and 75% of available valid data; (g) Soil moisture mean values modeled using GLM and 50% of available valid data.



377

378

379

380

381

Figure 9. Density distribution of mean soil moisture values along the study period for 741 pixels over the region interest. (a) ESA CCI and modelled data using OK with 100%, 75% and 50% of available valid data; (b) ESA CCI and modelled data using GLM with 100%, 75% and 50% of available valid data.

382 4. Discussion

383 Our results showed that OK and GLM techniques could be used as alternative approaches to
384 gap-filling in soil moisture data derived from ESA CCI product version 3.2. Our proposed methods
385 can be used either in conjunction with ancillary data as precipitation and temperature or using solely
386 the spatial distribution of soil moisture estimates derived from ESA CCI product. Furthermore, our
387 results show that spatial patterns and temporal relations between satellite and ground-truth data are
388 preserved by using OK, and can benefit from GLM approach, although the input data for each
389 method may be different.

390 Precipitation and minimum air temperature were the strongest correlated environmental
391 covariates with soil moisture (supplementary material S2). These relationships are likely influenced
392 by the grid size (0.25 degrees), as the spatial influence of precipitation and air temperature represents
393 regional and mesoscale climatic patterns [47]. Previous research showed that the increasing in spatial
394 resolution yields more detail in the meteorological information but just limited impacts on its
395 forecasting skill [48]. It is known that from plot to watershed scale soil texture and topography are
396 highly correlated with soil moisture [2,3], but these relationships may change at the coarse scale of
397 the ESA CCI soil moisture product. Thus, these features were not included as geophysical covariates
398 in our GLM approach.

399 Overall, our results provide support for OK and GLM as techniques to gap-fill spatial missing
400 values of satellite-derived soil moisture products. However, overall performance indicates that OK
401 represents a more reliable method for soil moisture gap-filling in comparison with GLM. Previous
402 studies have compared the advantages of OK for interpolation of spatial soil moisture and other soil
403 properties [49–52] but most analyses have been performed for spatially interpolating soil properties
404 based on field data [24,52–54]. OK has been regarded as an unbiased linear estimator [41] and our
405 results support it as a feasible approach due to the spatial scale of the original ESA CCI estimates
406 (0.25 degrees) under the gap scenarios tested in this work. At this coarse scale, soil moisture values
407 represent a quasi-continuous matrix that meets basic assumptions of Kriging analysis such as
408 stationarity [41] and spatial dependence [52]. OK also incorporates spatial autocorrelation by using
409 the variogram and providing the error variance estimation from predicted values, offering some
410 advantages over deterministic methods such as Inverse Distance Weighting (IDW), which may create
411 noisy fields in interpolation processes. As other Kriging methods, OK is an exact interpolator, which
412 ensures that values at sampled locations are exactly preserved. Thus, we aim to fill the spatial gaps
413 by modeling the entire region of interest, while preserving original values where data existed
414 previously. Additionally, OK performs value predictions based solely on spatial data distribution,
415 offering a suitable approach in cases where no well represented covariates datasets are available over
416 the region of interest as well as it compensates for data clustering [55]. Another evidence in support
417 for OK is the fact that the nugget-sill ratio was less than 0.25 in 99% of the fitted variograms, which
418 implies strong spatial dependence as discussed elsewhere [42].

419 In the case of GLM, this approach allowed us to explore the most evident relationships between
420 soil moisture in the upper layer of soil and the atmospheric factors that we found to be better
421 correlated (supplementary material S2). We followed a parsimonious principle by means of GLM
422 technique, applying the simplest model with the least assumptions before assuming relationships
423 that are more complex. This parsimonious reasoning and its applications to multivariate models has
424 been explored in other studies [56].

425 The evaluation of both OK and GLM approaches by means of cross-validation regarding their
426 prediction capacity for actual satellite data, shows similar correlation coefficients as reported by [53]
427 in spatial interpolation of soil moisture, and similar RMSE as reported by [52] for other soil properties.
428 Cross-validation technique has been commonly used in other similar studies [52,53] and offers and
429 initial insights of modeling techniques without considering ground-truth data for validation. Our
430 cross-validation strategy showed that OK better predicted soil moisture values rather than GLM, in
431 spite of pixel removal at different percentages. Regarding cross-validation for monthly grouped
432 values, neither OK nor GLM show an evident bias due to seasonality, as monthly correlation

433 coefficients and RMSE values systematically describe the same patterns found when using data from
434 the entire study period in a single dataset.

435 In spite of cross-validation results, ground-truth validation was performed to evaluate the
436 suitability of each method (OK and GLM) predicting missing values in the ESA CCI product. We
437 acknowledge the conceptual challenge of this data matching, and the need of balancing ground-truth
438 information in order to be representative of satellite-derived estimates. Representativeness
439 challenges in validation ESA CCI product have been also acknowledged previously [36]. Two main
440 problems are identified [36]. 1) Satellite sensors retrieve ground information from the upper soil layer
441 (0.5 – 5-cm depth), this layer is directly exposed to the atmosphere, therefore, its physical
442 characteristics may differ from the information provided by soil moisture sensors placed at 5-cm
443 depth or deeper. Thus, satellite estimates represent a more variable soil layer, different from soil at
444 deeper layers. 2) Even a spatially extensive soil moisture network cannot cover any area widely
445 enough, to provide scaling representativeness between point-scale measurements and satellite
446 estimates. Field measurements depict soil characteristics in the range of a few square decimeters,
447 while satellite products commonly cover a few kilometers per pixel (~27 km pixel sides in ESA CCI
448 product). In this regard, our work does not aim to provide strategies of accuracy assessment between
449 field measurements and satellite estimates as explored by [57]. We seek to reproduce the spatial soil
450 moisture patterns expressed by the satellite-derived soil moisture and its actual correlation with
451 ground-truth data.

452 As proposed by [57], the selection of reliable ground-truth stations and the definition of Core
453 Validation Sites (CSV) represent a step forward in the evaluation of remotely sensed soil moisture.
454 However, regarding the limited availability of ground stations providing soil moisture information,
455 we integrated all available ground-truth data for our region of interest instead of defining CSV. This
456 way, we took advantage of all available field soil moisture records over the region of interest. This
457 approach might introduce uncertainty, as neighboring stations within the same 0.25 degrees pixels
458 in some cases could be affected by different moisture conditions in a large area. However, as our
459 approach aims to reproduce the spatial distribution of soil moisture showed by the satellite estimates
460 based on the correlation with ground-truth data, we aim to retain all the variation offered by NASMD
461 stations.

462 In order to define the best-tested soil moisture prediction model to fill the gaps in ESA CCI
463 product, correlation founded with ground-truth data was set as reference for our proposed models
464 in every month of the study period. This yielded a more specific way to validate our proposed
465 methods regarding different soil moisture estimates conditions in every month of the ESA CCI
466 product. Given that our research aims to complete spatial information of ESA CCI, reference
467 correlation coefficients helped us to define which model, best reproduces the spatial pattern of the
468 original product. OK showed better results over GLM, as we found, higher the number of valid pixels
469 to shape the variogram parameters, closer the correlation coefficient to the reference. Furthermore,
470 OK performance does not significantly decreases even though valid pixel are artificially removed.
471 On the other hand, GLM correlation with ground-truth data, showed less similar values to the
472 reference, independently of the percentage of valid pixels removed.

473 Given that, OK and GLM performance for our region of interest does not fall very apart, GLM
474 can be an alternative approach in similar regions where satellite-derived soil moisture estimates are
475 spatially scarce or high clustered. As GLM relies more on predictors availability rather than spatial
476 distribution. Besides, when OK does not meet the best requirements, GLM can ingest data from
477 robust meteorological datasets [58,59] to obtain the geophysical covariates that we used in our
478 analysis. Based on the correlation coefficient between ESA CCI soil moisture product and NASMD
479 ground-truth data, we found that OK consistently better reproduces reference correlation coefficients
480 and RMSE values. Nevertheless, GLM correlation coefficients and RMSE values with NASMD do not
481 significantly decrease from the reference, which still makes this method an alternative approach to
482 gap-filling. Finally, the analysis of the mean soil moisture spatial patterns along the study period
483 showed that OK outputs consistently better reproduced the spatial patterns in the original ESA CCI

484 product. This can be visually distinguished on the mean soil moisture maps, as well as in the density
485 distribution of the original product in comparison with both OK and GLM outputs.

486 We acknowledge that OK represents the best-tested method for soil moisture prediction and
487 gap-filling of the ESA CCI product over our region of interest, based on the analysis of the monthly
488 mean values from January 2000 to September 2012. The application of this method in other regions
489 and under different conditions, should consider availability and distribution of soil moisture
490 estimates. Since in large discontinuous areas, stationary can be wrongly assumed, yielding high
491 uncertainty in predicted values. Although ESA CCI soil moisture product has released a new version
492 (4.4), we consider the approaches proposed in this work as an alternative strategy to improve the gap
493 filling process, as the new version still shows large areas with gaps (supplementary material S1).

494 In future research, it is necessary to explore ESA CCI gap-filling over larger areas such as the
495 conterminous United States, where well spatially represented meteorological datasets are available
496 and different scenarios of gaps distribution can be tested. Daily data must be also incorporated, as
497 this is the temporal resolution in which original soil moisture estimates are delivered. Thus, opening
498 the possibility to operationally filling the gaps in the original soil moisture estimates provided by
499 ESA CCI product. These implementations represent an upscaling need in computational capacities,
500 therefore, High Performance Computing (HPC) techniques must be considered.

501 5. Conclusions

502 For the region of interest, linear geostatistics techniques offer a suitable approach to fill the soil
503 moisture spatial gaps of the ESA CCI product (version 3.2). Although version 4.4 follows different
504 strategies to fill data gaps, our research highlights the incorporation of spatial distribution of soil
505 moisture, as well as the use of geophysical covariates to model-missing values. Selected geophysical
506 covariates to model soil moisture in this study, i.e. precipitation and minimum air temperature, can
507 be easily integrated due to their historical availability across larger regions e.g. conterminous United
508 States (CONUS). Selected region of interest provided a spatially extent set of valid pixels from
509 January 2000 to September 2012, which allowed us to test our proposed methods under different
510 scenarios of gap presence, due to natural conditions as well as artificial pixel removal.

511 Ordinary Kriging method does not need to use any additional covariates as it is built upon the
512 spatial distribution of soil moisture data, however this method can be inconclusive over areas where
513 reference data is highly sparse or clustered (i.e., data scenarios where we found weak spatial structure
514 on satellite soil moisture). General Linear Models on the other hand, offer an alternative to spatially
515 model soil moisture and fill the gaps in the ESA CCI product, however their performance is lower
516 than OK. As we found in this research, soil moisture at coarse scale can be significantly correlated to
517 covariates such as precipitation and minimum air temperature, which can be easily ingested by
518 predicting models over most of CONUS.

519 Derived from cross-validation for each method and specific percentage of available data, both
520 methods—Ordinary Kriging and General Linear Models—showed significant prediction
521 performance for soil moisture data. However, as we intended to reproduce the soil moisture spatial
522 patterns of the ESA CCI product and its relationship with ground-truth soil moisture data, we
523 considered field validation as the best approach to find the most suitable gap-filling method.

524 Besides offering information for a wide variety of applications by itself, spatially complete soil
525 moisture information covering large areas can also be related to point-based soil moisture networks
526 to jointly monitoring ecological processes. Thus, soil moisture gap-filled data can yield a better
527 understanding of its role in water and carbon cycles, with important implications in plant and soil
528 respiration, or plant growth. Therefore, influencing our capacity to predict climate change signals in
529 soil moisture estimates from the regional to the global scale.

530 **Supplementary Materials:** Supplementary materials S1, S2 and S3 are submitted with this manuscript.

531 **Author Contributions:** R.L.L., M.G. and R.V. conceived and designed the research. R.L.L. and M.G. developed
532 the code for processing and analyzing the data. R.L.L. wrote the first draft of the manuscript with input from

533 R.V. All authors contributed with interpretation of the results, reviewed, and approved the manuscript. R.V. and
534 M.T. supervised and coordinated the research team.

535 **Funding:** This study was funded by a University of Delaware Strategic Initiative research grant and the National
536 Science Foundation (OAC grant#1724843).

537 **Acknowledgments:** We thank Inder Tecuapetla for his input on the conceptual analysis of spatio-temporal
538 correlation, and Paula Olaya and Joe Teague for their comments to improve this work.

539 **Conflicts of Interest:** “The authors declare no conflict of interest.”

540 References

- 541 1. Ward, S. *The Earth observation handbook*; ESA Communication Production Office: Noordwijk, The
542 Netherlands, 2008.
- 543 2. Koster, R. D.; Suarez, M. J. Soil Moisture Memory in Climate Models. *J. Hydrometeorol.* **2001**, *2*, 558–570,
544 doi:10.1175/1525-7541(2001)002<0558:SMMICM>2.0.CO;2.
- 545 3. Seneviratne, S. I.; Corti, T.; Davin, E. L.; Hirschi, M.; Jaeger, E. B.; Lehner, I.; Orlowsky, B.; Teuling, A. J.
546 Investigating soil moisture-climate interactions in a changing climate: A review. *Earth-Science Rev.* **2010**, *99*,
547 125–161, doi:10.1016/j.earscirev.2010.02.004.
- 548 4. Meehl, G. A.; Washington, W. M. A Comparison of Soil-Moisture Sensitivity in Two Global Climate
549 Models. *J. Atmos. Sci.* **1988**, *45*, 1476–1492.
- 550 5. Engman, E. T. Applications of microwave remote sensing of soil moisture for water resources and
551 agriculture. *Remote Sens. Environ.* **1991**, *35*, 213–226, doi:10.1016/0034-4257(91)90013-V.
- 552 6. Narasimhan, B.; Srinivasan, R. Development and evaluation of Soil Moisture Deficit Index (SMDI) and
553 Evapotranspiration Deficit Index (ETDI) for agricultural drought monitoring. *Agric. For. Meteorol.* **2005**, *133*,
554 69–88, doi:10.1016/j.agrformet.2005.07.012.
- 555 7. Davidson, E. A.; Belk, E.; Boone, R. D. Soil water content and temperature as independent or confounded
556 factors controlling soil respiration in a temperate mixed hardwood forest. *Glob. Chang. Biol.* **1998**, *4*, 217–
557 227, doi:10.1046/j.1365-2486.1998.00128.x.
- 558 8. Williams, C. A.; Albertson, J. D. Soil moisture controls on canopy-scale water and carbon fluxes in an
559 African savanna. *Water Resour. Res.* **2004**, *40*, 1–14, doi:10.1029/2004WR003208.
- 560 9. Dorigo, W. A.; Wagner, W.; Hohensinn, R.; Hahn, S.; Paulik, C.; Xaver, A.; Gruber, A.; Drusch, M.;
561 Mecklenburg, S.; Van Oevelen, P.; Robock, A.; Jackson, T. The International Soil Moisture Network: A data
562 hosting facility for global in situ soil moisture measurements. *Hydrol. Earth Syst. Sci.* **2011**, *15*, 1675–1698,
563 doi:10.5194/hess-15-1675-2011.
- 564 10. Dorigo, W. A.; Xaver, A.; Vreugdenhil, M.; Gruber, A.; Hegyiová, A.; Sanchis-Dufau, A. D.; Zamojski, D.;
565 Cordes, C.; Wagner, W.; Drusch, M. Global Automated Quality Control of In Situ Soil Moisture Data from
566 the International Soil Moisture Network. *Vadose Zo. J.* **2013**, *12*, 0, doi:10.2136/vzj2012.0097.
- 567 11. Dorigo, W. A.; Gruber, A.; De Jeu, R. A. M.; Wagner, W.; Stacke, T.; Loew, A.; Albergel, C.; Brocca, L.;
568 Chung, D.; Parinussa, R. M.; Kidd, R. Evaluation of the ESA CCI soil moisture product using ground-based
569 observations. *Remote Sens. Environ.* **2015**, *162*, 380–395, doi:10.1016/j.rse.2014.07.023.
- 570 12. Robock, A.; Mu, M.; Vinnikov, K.; Trofimova, I. V.; Adamenko, T. I. Forty-five years of observed soil
571 moisture in the Ukraine: No summer desiccation (yet). *Geophys. Res. Lett.* **2005**, *32*, 1–5,
572 doi:10.1029/2004GL021914.
- 573 13. Martínez-Fernández, J.; Ceballos, A. Temporal Stability of Soil Moisture in a Large-Field Experiment in
574 Spain. *Soil Sci. Soc. Am. J.* **2003**, *67*, 1647, doi:10.2136/sssaj2003.1647.
- 575 14. Schaefer, G. L.; Cosh, M. H.; Jackson, T. J. The USDA Natural Resources Conservation Service Soil Climate
576 Analysis Network (SCAN). *J. Atmos. Ocean. Technol.* **2007**, *24*, 2073–2077, doi:10.1175/2007JTECHA930.1.
- 577 15. Quiring, S. M.; Ford, T. W.; Wang, J. K.; Khong, A.; Harris, E.; Lindgren, T.; Goldberg, D. W.; Li, Z. The
578 North American Soil Moisture Database: Development and Applications. *Bull. Am. Meteorol. Soc.* **2016**, *97*,
579 1441–1459, doi:10.1175/BAMS-D-13-00263.1.
- 580 16. Entekhabi, D.; Njoku, E. G.; O'Neill, P. E.; Kellogg, K. H.; Crow, W. T.; Edelstein, W. N.; Entin, J. K.;
581 Goodman, S. D.; Jackson, T. J.; Johnson, J.; Kimball, J.; Piepmeier, J. R.; Koster, R. D.; Martin, N.; McDonald,
582 K. C.; Moghaddam, M.; Moran, S.; Reichle, R.; Shi, J. C.; Spencer, M. W.; Thurman, S. W.; Tsang, L.; Van
583 Zyl, J. The soil moisture active passive (SMAP) mission. *Proc. IEEE.* **2010**, *98*, 704–716,
584 doi:10.1109/JPROC.2010.2043918.

- 585 17. ESA SMOS Mission summary Available online: [https://earth.esa.int/web/guest/missions/esa-eo-](https://earth.esa.int/web/guest/missions/esa-eo-missions/smos/mission-summary)
586 [missions/smos/mission-summary](https://earth.esa.int/web/guest/missions/esa-eo-missions/smos/mission-summary) (accessed on Jul 13, 2018).
- 587 18. Dorigo, W.; Wagner, W.; Albergel, C.; Albrecht, F.; Balsamo, G.; Brocca, L.; Chung, D.; Ertl, M.; Forkel, M.;
588 Gruber, A.; Haas, E.; Hamer, P. D.; Hirschi, M.; Ikonen, J.; de Jeu, R.; Kidd, R.; Lahoz, W.; Liu, Y. Y.; Miralles,
589 D.; Mistelbauer, T.; Nicolai-Shaw, N.; Parinussa, R.; Pratola, C.; Reimer, C.; van der Schalie, R.; Seneviratne,
590 S. I.; Smolander, T.; Lecomte, P. ESA CCI Soil Moisture for improved Earth system understanding: State-
591 of-the art and future directions. *Remote Sens. Environ.* **2017**, *203*, 185–215, doi:10.1016/j.rse.2017.07.001.
- 592 19. Topp, G. C.; Davis, J. L.; Annan, A. P. Electromagnetic Determination of Soil Water Content: Measurements
593 in Coaxial Transmission Lines. *Water Resour. Res.* **1980**, *16*, 574–582, doi:10.1029/WR016i003p00574.
- 594 20. Chung, D.; Dorigo, W.; De Jeu, R.; Kidd, R.; Wagner, W. Product Specification Document (PSD) D.1.2.1
595 Version 4.4, 2018, 49.
- 596 21. Gruber, A.; Dorigo, W. A.; Crow, W.; Wagner, W. Triple Collocation-Based Merging of Satellite Soil
597 Moisture Retrievals. *IEEE Trans. Geosci. Remote Sens.* **2017**, *55*, 6780–6792, doi:10.1109/TGRS.2017.2734070.
- 598 22. Wang, G.; Garcia, D.; Liu, Y.; de Jeu, R.; Johannes Dolman, A. A three-dimensional gap filling method for
599 large geophysical datasets: Application to global satellite soil moisture observations. *Environ. Model. Softw.*
600 **2012**, *30*, 139–142, doi:10.1016/j.envsoft.2011.10.015.
- 601 23. Kondrashov, D.; Ghil, M. Spatio-temporal filling of missing points in geophysical data sets. *Nonlinear*
602 *Process. Geophys.* **2006**, *13*, 151–159.
- 603 24. DeLiberty, T. L.; Legates, D. R. Spatial Variability and Persistence of Soil Moisture in Oklahoma. *Phys.*
604 *Geogr.* **2008**, *29*, 121–139, doi:10.2747/0272-3646.29.2.121.
- 605 25. Hengl, T.; Heuvelink, G. B. M.; Stein, A. A generic framework for spatial prediction of soil variables based
606 on regression-kriging. *Geoderma.* **2004**, *120*, 75–93, doi:10.1016/j.geoderma.2003.08.018.
- 607 26. Cressie, N. The origins of kriging. *Math. Geol.* **1990**, *22*, 239–252, doi:10.1007/BF00889887.
- 608 27. Oliver, M. A.; Webster, R. *Basics Steps in Geostatistics: The Variogram and Kriging*; Springer: New York, NY,
609 2015.
- 610 28. Brock, F. V.; Crawford, K. C.; Elliott, R. L.; Cuperus, G. W.; Stadler, S. J.; Johnson, H. L.; Eilts, M. D. The
611 Oklahoma Mesonet: A Technical Overview. *J. Atmos. Ocean. Technol.* **1995**, *12*, 5–19.
- 612 29. Commission for Environmental Cooperation. 2010 Land Cover of North America at 30 meters, Ed. 1. 2017.
613 [http://www.cec.org/tools-and-resources/north-american-environmental-atlas/land-cover-and-land-cover-](http://www.cec.org/tools-and-resources/north-american-environmental-atlas/land-cover-and-land-cover-change)
614 [change](http://www.cec.org/tools-and-resources/north-american-environmental-atlas/land-cover-and-land-cover-change).
- 615 30. Llamas, R. M. R. M.; Bonifaz, R.; Valdés, M.; Riveros-Rosas, D.; Leyva-Contreras, A. Spatial and temporal
616 variations of atmospheric aerosol optical thickness in northwestern Mexico. *Geofis. Int.* **2013**, *52*, 321–341,
617 doi:10.1016/S0016-7169(13)71480-6.
- 618 31. Thornton, M. M.; Thornton, P. E.; Wei, Y.; Mayer, B. W.; Cook, R. B.; Vose, R. S. Daymet: Monthly Climate
619 Summaries on a 1-km Grid for North America, Version 3. ORNL DAAC, Oak Ridge, Tennessee, USA, 2018.
620 <https://doi.org/10.3334/ORN LDAAC/1345>.
- 621 32. Parker, J. A.; Kenyon, R. V.; Troxel, D. E. Comparison of Interpolating Methods for Image Resampling.
622 *IEEE Trans. Med. Imaging.* **1983**, MI-2, 31–39, doi:10.1109/TMI.1983.4307610.
- 623 33. Soil Survey Staff. Gridded Soil Survey Geographic (gSSURGO) Database for the Conterminous United
624 States. United States Department of Agriculture, Natural Resources Conservation Service, 2016. Available
625 on line at <https://gdg.sc.egov.usda.gov/>.
- 626 34. Bertermann, D.; Bialas, C.; Morper-Busch, L.; Klug, H.; Rohn, J.; Stollhofen, H.; Psyk, M.; Jaudin, F.;
627 Maragna, C.; Einarsson, G. M.; Vikingsson, S.; Orosz, L.; Jordan, G.; Vijiya, A.-M.; Lewis, M.; Lawley, R. S.;
628 Latham, A.; Declercq, P.-Y.; Petittler, E.; Zacherl, A.; Arvanitis, A.; Stefouli, M. ThermoMap - An Open-
629 Source Web Mapping Application for Illustrating the very Shallow Geothermal Potential in Europe and
630 selected Case Study Areas. *Eur. Geotherm. Congr.* **2013**, 1–8.
- 631 35. Conrad, O.; Bechtel, B.; Bock, M.; Dietrich, H.; Fischer, E.; Gerlitz, L.; Wehberg, J.; Wichmann, V.; Böhner,
632 J. System for Automated Geoscientific Analyses (SAGA) v.2.1.4. *Geosci. Model. Dev.* **2015**, *8*, 1991–2007,
633 doi:10.5194/gmd-8-1991-2015.
- 634 36. ESA CCI ESA Soil Moisture CCI Validation, Available online: [https://www.esa-soilmoisture-](https://www.esa-soilmoisture-cci.org/validation)
635 [cci.org/validation](https://www.esa-soilmoisture-cci.org/validation) (accessed on Jul 1, 2019).
- 636 37. Kutner, M. H.; Nachtsheim, C. J.; Neter, J.; Li, W. *Applied Linear Statistical Models*; 5th ed.; McGraw-Hill:
637 New York, 2005.

- 638 38. Jung, C.; Lee, Y.; Cho, Y.; Kim, S. A study of spatial soil moisture estimation using a multiple linear
639 regression model and MODIS land surface temperature data corrected by conditional merging. *Remote*
640 *Sens.* **2017**, *9*, 1–20, doi:10.3390/rs9080870.
- 641 39. Cai, Y.; Zheng, W.; Zhang, X.; Zhangzhong, L.; Xue, X. Research on soil moisture prediction model based
642 on deep learning. *PLoS One.* **2019**, *14*, 1–19, doi:10.1371/journal.pone.0214508.
- 643 40. Hiemstra, P. H.; Pebesma, E. J.; Twenhöfel, C. J. W.; Heuvelink, G. B. M. Real-time automatic interpolation
644 of ambient gamma dose rates from the Dutch radioactivity monitoring network. *Comput. Geosci.* **2009**, *35*,
645 1711–1721, doi:10.1016/j.cageo.2008.10.011.
- 646 41. Isaaks, E. H.; Srivastava, R. M. Ordinary Kriging. In *Applied Geostatistics*; Oxford University Press: New
647 York, USA, 1989; pp. 278–322.
- 648 42. Cambardella, C. A.; Moorman, T. B.; Parkin, T. B.; Karlen, D. L.; Novak, J. M.; Turco, R. F.; Konopka, A. E.
649 Field-Scale Variability of Soil Properties in Central Iowa Soils. *Soil Sci. Soc. Am. J.* **1994**, *58*, 1501–1511,
650 doi:10.2136/sssaj1994.03615995005800050033x.
- 651 43. Kuhn, M. caret: Classification and Regression Training. R package version 6.0-71. 2016. [https://CRAN.R-](https://CRAN.R-project.org/package=caret)
652 [project.org/package=caret](https://CRAN.R-project.org/package=caret)
- 653 44. Stein, M. L. *Interpolation of Spatial Data, Some Theory for Kriging*; Springer: Chicago, IL, USA, 1999.
- 654 45. Taylor, K. E. Summarizing multiple aspects of a model performance in a single diagram. *J. Geophys. Res.*
655 **2001**, *106*, 7183–7192, doi:10.1029/2000JD900719.
- 656 46. Lemon, J. Plotrix: a package in the red light district of R. *R-News.* **2006**, *6*, 8–12.
- 657 47. Tang, C.; Chen, D. Interaction between Soil Moisture and Air Temperature in the Mississippi River Basin.
658 *J. Water Resour. Prot.* **2017**, *9*, 1119–1131, doi:10.4236/jwarp.2017.910073.
- 659 48. Salathé Jr., E. P.; Steed, R.; Mass, C. F.; Zahn, P. H. A High-Resolution Climate Model for the U.S. Pacific
660 Northwest: Mesoscale Feedbacks and Local Responses to Climate Change. *J. Clim.* **2008**, *21*, 5708–5726,
661 doi:10.1175/2008JCLI2090.1.
- 662 49. Ding, Y.; Wang, Y.; Miao, Q. Research on the spatial interpolation methods of soil moisture based on GIS.
663 Proc. of Intl. Conf. on. Sci. and Tech., Nanjing, China, March 26-28, 2011, 709–711,
664 doi:10.1109/ICIST.2011.5765344.
- 665 50. Chen, H.; Fan, L.; Wu, W.; Liu, H-B. Comparison of spatial interpolation methods for soil moisture and its
666 application for monitoring drought. *Environ. Monit. Assess.* **2017**, *189*, doi:10.1007/s10661-017-6244-4.
- 667 51. Zhang, M.; Li, M.; Wang, W.; Liu, C.; Gao, H. Temporal and spatial variability of soil moisture based on
668 WSN. *Math. Comput. Model.* **2013**, *58*, 826–833, doi:10.1016/j.mcm.2012.12.019.
- 669 52. Cruz-Cárdenas, G.; López-Mata, L.; Ortiz-Solorio, C. A.; Villaseñor, J. L.; Ortiz, E.; Silva, J. T.; Estrada-
670 Godoy, F. Interpolation of Mexican soil properties at a scale of 1:1,000,000. *Geoderma.* **2014**, *213*, 29–35,
671 doi.org/10.1016/j.geoderma.2013.07.014.
- 672 53. De Benedetto, D.; Castrignanò, A.; Quarto, R. A Geostatistical Approach to Estimate Soil Moisture as a
673 Function of Geophysical Data and Soil Attributes. *Procedia Environ. Sci.* **2013**, *19*, 436–445,
674 doi:10.1016/j.proenv.2013.06.050.
- 675 54. Abuduwaili, J.; Tang, Y.; Abulimiti, M.; Liu, D.; Ma, L. Spatial distribution of soil moisture, salinity and
676 organic matter in Manas River watershed, Xinjiang, China. *J. Arid Land.* **2012**, *4*, 441–449,
677 doi:10.3724/SP.J.1227.2012.00441.
- 678 55. Brusilovskiy, E. Spatial Interpolation: A Brief Introduction Available online: [http://www.bisolutions.us/A-](http://www.bisolutions.us/A-Brief-Introduction-to-Spatial-Interpolation.php)
679 [Brief-Introduction-to-Spatial-Interpolation.php](http://www.bisolutions.us/A-Brief-Introduction-to-Spatial-Interpolation.php) (accessed on Oct 22, 2018).
- 680 56. Seasholtz, M. B.; Kowalski, B. The parsimony principle applied to multivariate calibration. *Anal. Chim. Acta.*
681 **1993**, *277*, 165–177, doi:10.1016/0003-2670(93)80430-S.
- 682 57. Colliander, A.; Jackson, T. J.; Bindlish, R.; Chan, S.; Das, N.; Kim, S. B.; Cosh, M. H.; Dunbar, R. S.; Dang,
683 L.; Pashaian, L.; Asanuma, J.; Aida, K.; Berg, A.; Rowlandson, T.; Bosch, D.; Caldwell, T.; Caylor, K.;
684 Goodrich, D.; al Jassar, H.; López-Baeza, E.; Martínez-Fernández, J.; González-Zamora, A.; Livingston, S.;
685 McNairn, H.; Pacheco, A.; Moghaddam, M.; Montzka, C.; Notarnicola, C.; Niedrist, G.; Pellarin, T.; Prueger,
686 J.; Pulliainen, J.; Rautiainen, K.; Ramos, J.; Seyfried, M.; Starks, P.; Su, Z.; Zeng, Y.; van der Velde, R.;
687 Thibeault, M.; Dorigo, W.; Vreugdenhil, M.; Walker, J. P.; Wu, X.; Monerris, A.; O'Neill, P. E.; Entekhabi,
688 D.; Njoku, E. G.; Yueh, S. Validation of SMAP surface soil moisture products with core validation sites.
689 *Remote Sens. Environ.* **2017**, *191*, 215–231, doi:10.1016/j.rse.2017.01.021.

- 690 58. Menne, M. J.; Durre, I.; Vose, R. S.; Gleason, B. E.; Houston, T. G. An Overview of the Global Historical
691 Climatology Network-Daily Database. *J. Atmos. Ocean. Technol.* **2012**, *29*, 897–910, doi:10.1175/JTECH-D-11-
692 00103.1.
- 693 59. Fick, S. E.; Hijmans, R. J. WorldClim 2: new 1-km spatial resolution climate surfaces for global land areas.
694 *Int. J. Climatol.* **2017**, *37*, 4302–4315, doi:10.1002/joc.5086.
695